OXYGEN REDUCTION ON $Cu_{1.4}Mn_{1.6}O_4$ SPINEL PARTICLES COMPOSITE ELECTRODES EFFECT OF PARTICLES SIZE

*ANDRES ESPEJO, JUAN ORTIZ, EDMUNDO RIOS, FRANCISCO HERRERA, DANIELA ALBURQUENQUE, JUAN LUIS GAUTIER**

Departamento de Química de los Materiales, Facultad de Química y Biología, Universidad de Santiago de Chile, Av. L.B. O'Higgins 3363, Santiago, Chile

ABSTRACT

The oxygen reduction reaction (orr) was studied on CG/PPy/PPy(Ox)/PPy and CG/paint/CC(Ox)PPy composite electrodes, CG representing conducting glass, PPy polypyrrole, CC carbon cloth and Ox mixed valence spinel oxide particles of transition metals $Cu_{1.4}Mn_{1.6}O_4$ in 0.2 M KCl pH = 9.2, at room temperature. PPy is electrochemically polymerized and serves as a protective layer to dispersed oxide particles in the carbon cloth.

Oxide particles size varied from 7.6 to 11.2 µm. The orr takes place on the oxide particles with formation of hydrogen peroxide which diffuses to electrolyte solution. The amount of peroxide ions produced was detected using the rotating ring-disk electrode technique and determined indirectly by iodine spectroscopy. The peroxide ions production depends strongly on the oxide particle size.

Keywords: Copper manganites, Spinel oxide, Composite electrode, Polypyrrole, Oxygen electroreduction.

INTRODUCTION

The importance of the cathodic oxygen reduction reaction (orr) to water either directly or indirectly via hydrogen peroxide is widely recognized due to their applications such as oxygen electrode in fuel cells, lithium-air batteries, wastewater treatments and, organic and inorganic synthesis. In fuel cells the orr is the only employed reaction to accept electrons from chemicals such as methanol, ethanol or other molecules[1] and it is considered essential in lithium air batteries that corresponds to fuel of the positive electrode[2]. The ion peroxide, HO_2^-, is an oxidant for organic substances and is particularly powerful to remove of organics pollutants from industrial wastewater in presence of electrogenerated Fenton´s reagent[3]. However, the sluggish kinetics of orr significantly limits the efficiency of the electrochemical energy conversion[4] and need of suitable and inexpensive catalyst alternatives. Among the new catalysts developed for orr, manganese oxide composite have attracted recently much attention[5].

Mixed valence oxides of transition metal with a spinel structure are important class of metal oxides that crystallize in the spinel structure. The unit cell can be represented by 8 groups AB_2O_4 where A is a cation tetrahedrally coordinated with oxygen and B a cation octahedrally coordinated with oxygen. Spinel oxides have been extensively investigated as orr catalyst due to its high activity, lower cost, and high stability[6,7].

In previous research work it has been confirmed the feasibility for the orr of multilayer composite electrodes having the structure GC/PPy/PPy(Ox)/PPy (GC, glassy carbon, PPy, polypyrrole, Ox, oxide) Ox being a spinel oxide of copper and manganese[8], $Cu_{1.4}Mn_{1.6}O_4$, or nickel and cobalt[9,10], $Ni_{0.3}Co_{2.7}O_4$, or iron and cobalt[11], $CoFe_2O_4$. In the composite electrode, particles of oxide electrocatalyst, Ox, are sandwiched like between two PPy layers. It is important to remark that the incorporation of metal oxide particles is facilitated by pzc located a low pH values, such is the case of Cu-Mn oxide with pHz = 2.6[12]. Remarkable electrocatalytical activity due to electrodes GC/PPy/PPy($Cu_{1.4}Mn_{1.6}O_4$)/PPy even in acid medium at negative potentials was investigated by us[13]. Previous studies[14] on orr electrocatalysis using the spinel oxides system $Cu_xMn_{3-x}O_4$ $1.0 \leq x \leq 1.4$ showed a progressive increment of oxygen reduction rate which is related to copper concentration, being maximal to $Cu_{1.4}Mn_{1.6}O_4$.

Studies using XPS, Mn K-edge XANES and EXAFS[15] techniques shown that the composite electrode structure prior to the incorporation of the oxide into the PPy matrix, contains Cu^+, Cu^{2+}, Mn^{3+}, Mn^{4+}. However, when the oxide is incorporated into de PPy matrix , two important features were observed : (i) the Cu^+ suffers dismutation to give Cu^{2+} and Cu^o metallic giving place to the formation of a large number of vacancies and (ii) Mn is present as Mn^{3+} and Mn^{4+} occupying octahedral sites while the cooper occupies tetrahedral sites in a disordered spinel structure. On the other hand, when the composite electrodes are polarized at - 0.45V/SCE in solution at acid pH, the presence of Cu^o and Cu^{2+} and Mn^{3+}/Mn^{4+} ratio were confirmed, although the manganese ratio is different from the original found in the unreacted fresh electrodes[16]. It is widely accepted that the B-sites are the most peripheral sites in spinels.

Conductive polymers (PANI, PY, PT, and derivates) and oxidized metallic particles deposited on carbons tends to enhance the final capacity of electrochemical energy storage through fast faradic reactionss[17]. It is well known that carbon materials with high specific surface area, such as activated carbon, carbon fiber, carbon cloth, and carbon nanotubes are usually used as electrode materials for electrochemical devices[18-25]. Recently it had been reported that the tridimensional electrode of high area based on carbon cloth used to charge $Cu_{1.4}Mn_{1.6}O_4$ as electrocatalyst exhibits excellent electrocatalytic reactivity towards orr[26].

Another factor that becomes important with dispersed electrocatalyst particles for oxygen reduction is the influence of the particle size on reduction kinetics. As the electrocatalyst particle becomes smaller, a large fraction of the total number of atoms in the particle is associated with surface sites, and the properties of these surface cations may differ from those of surface cations in bulk oxides concerning the adsorption properties. Specific sites on oxide structure considered as active sites may enhanced nearby sites activity. .

The aim of this research work was to determine the parameters that control the formation and yields of oxygen peroxide obtained from the orr on multilayer composite CG/PPy/PPy/$Cu_{1.4}Mn_{1.6}O_4$/PPy and CG/CC/$Cu_{1.4}Mn_{1.6}O_4$/PPy electrodes.

EXPERIMENTAL

$Cu_{1.4}Mn_{1.6}O_4$ mixed valence oxide particles were synthesized in polycrystalline form by thermal decomposition of coprecipitated hydroxides, as reported elsewhere[14]. Briefly, an excess quantity of NaOH was slowly added to a mixed solution of $MnSO_4$ x H_2O + $CuSO_4$ in stoichiometric proportions. All the reagents were of analytical grade (Aldrich). The formed coprecipitate was rinsed abundantly with double distilled water, drying at 120ºC for 4 h, then ground and heated at 590ºC in air during 48h. After quenching in air, the resulting powder was more finely ground using an automatic mill, RM RETSCH mill for different times in order to obtain different sizes. Subsequently each sample was treated at 530ºC during 24 h in air. Their actual Cu and Mn concentrations were checked by EDAX corresponding to the preparation stoichiometry. Phase purity of the oxides before and after embedment in the composite electrodes was checked by powder X-ray diffraction (XRD) using Ni-filtered Cu Kα radiation (λ = 0.154056 nm). The a cell parameter was 0.8305 nm as reported[14].

Platelets of conductive glass (CG) were prepared using the chemical spray pyrolysis technique. On a non-conductive glass (2.5 cm x 1cm x 0.1cm) successive layers of 0.2M $SnCl_4$ solution doped with 0.1M NH_4F were sprayed on the substrate placed at 420ºC, controlling the surface temperature with an infrared pyrometer (Scotchtrak 3M). The SnO_2 deposit obtained on the platelets was checked using XRD analysis and their conductivity determined by an ohmmeter.

Manufacture of composite electrodes.

The preparation of the composite electrode CG/CC/$Cu_{1.4}Mn_{1.6}O_4$)/PPy involved three consecutive steps. The first step corresponds to the aqueous

 e-mail: juan.gautier@usach.cl

electropolymerization of pyrrole (Aldrich, previously distilled under Ar atmosphere) carried out in a three electrode cell containing 20 ml of 0.1M Py + 0.2M KCl solution at 20 $mAcm^{-2}$ during 35s. Conductive glass Platelets(CG) were the working electrodes with a surface area of 1 cm2. Prior to electropolymerization, the electrodes were slightly polished on a rotating disk coated with 1µm diamond particles (IPS4A-1MIC,ESCIL), then washed rigorously with deionized water in an ultrasound bath. The auxiliary and reference electrodes were of a cylindrical Pt mesh and a saturated calomel electrode (SCE) respectively. The carbon cloth (CC) E-TEK was cut having the same size as the CG. To obtain an efficient and firm electrical contact between the surface of CG electrodes and CC, graphite conductive paint has been used (D-LTA).

The use of carbon cloth can increment even further the dispersion and the utilization of the active catalyst, thereby improving its catalytic activity than PPy layer. In the second step, a suspended amount of oxide in solution (7.5 gL^{-1}) was pipetted onto the CC, which was penetrated by the solution. In order to standardize the dispersed oxide particles in the CC, the electrodes were placed in a heated oven at 80ºC to allow the total removal of the solvents. In the third step, the outer PPy layer was deposited galvanostatically at 20 mA for 75s using an electrolytical bath prepared with a mixture of 0.2M KCl (Aldrich) and 0.1M Py solution. The solution was deoxygenated for 1h before use by bubbling Ar and maintained under Ar atmosphere during the electropolymerization of pyrrole. For comparison, another type of electrode was used in which the carbon cloth was replaced by a layer of polypirrol containing the oxide particles. The oxide particles were sandwiched in CG/PPy/PPy($Cu_{1.4}Mn_{1.6}O_4$)/PPy electrode composite. PPy electrodeposited on CG yielding the CG/PPy (first portion of the composite electrode) was performed at RT using 20 mL of aqueous solution containing 0.1M Py and 0.2M KCl at 20 mA for 25s. The thickness of the PPy film was controlled by coulometry. In the second step, the GC/PPy structure was placed in 40mL of a solution containing 0.1MPy + 0.2M KCl + $Cu_{1.4}Mn_{1.6}O_4$ at a mass concentration 7.5gL^{-1} which was electrodeposited at 20$mAcm^{-2}$ for 180s, giving rice to the CG/PPy/PPy(Ox), second part of the electrode composite. Finally, a protective layer of PPy (third layer) was added using 20 mL of aqueous solution containing 0.1MPy + 0.2MKCl. The electropolimerizations were carried out with a Wenking PGS potentio-galvano scan. CG/CC/PPy was prepared in similar fashion using the same current density, electrolyte concentration, time of electrochemical reactions, without mixed oxide to confirm the findings regarding their electrochemical behaviour[24].

The electrochemical behavior of the composite electrodes was studied at RT in 0.2 M KCl solution, pH = 9.2 using a double-walled three electrode cell, where the working electrode was placed in concentric manner with respect the cylinder Pt-gauze counter-electrode. Oxygen was bubbled into the solution for 10 min prior to use, and maintained under an O_2 atmosphere for the duration of experiment. Stationary potentiostatic curves (1mVs^{-1}) were obtained using a Voltalab PGZ Radiometer potentiostat coupled to a computer.

Quantities of hydrogen peroxide generated at -0.6V/ECS were indirectly analyzed from the amounts of iodine, I_2, produced from the oxidation of iodine ion as reported before by us[10]. Free iodine was titrated by uv-vis spectrometry at λ = 352 nm using a calibration curve.

Manufacture of disk-ring electrode.

Firstly, a conducting pellet was prepared using graphite UCAR and suspension of Teflon (Du Pont) in the ratio 80:20 w/w from a paste obtained with the help of isobutyl alcohol. This paste acquires a cylindrical shape by pressure at 0.5T cm^{-2} during 15 min, which was thermally treated 2h at 350ºC obtaining hard and compact discs of 0.12 cm^2 area and 1mm thickness. CC having the same diameter was fixed with conductive glue on the carbon disk surface placed on working electrode. Then a suspension of oxide was added to the CC and sealed with a layer of PPY. The discs were the working electrodes of a rotating ring-disk electrode Tacussel.EAD with Pt ring. The HO_2^- formation from O_2 reduction using the electrolytic solution already indicated was studied measuring both the disk and ring current as a function of applied potential obtained using a bipotentiostat (Pine Co. RD3) and an electronic interface coupled to computer. Rotation rate of electrode was varied from 500 to 3000 rpm.

RESULTS AND DISCUSSION

Oxide particles size.

Figure 1 shows the dependence of the oxide particles size as a function of milling time. The particles size obtained by SEM was determined using the image software j[27]. It is observed that after 30h milling the mean particle size decreases by 60%. In the case of smaller oxide particles (7.6 µm), a 25% is placed between 4-6 µm as showed on the size distribution (Fig 2).

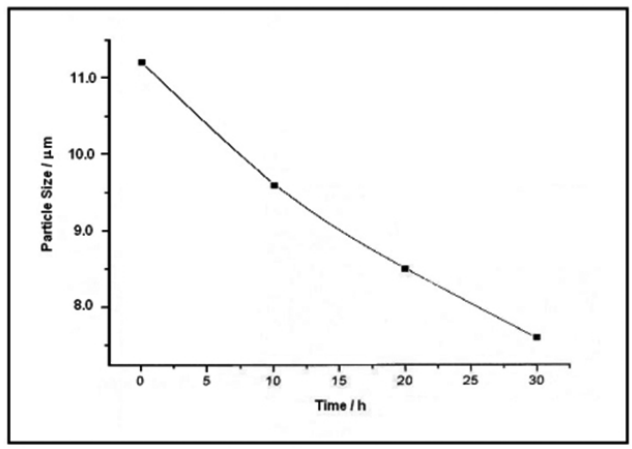

Fig.1. Average oxide particles size vs. milling time.

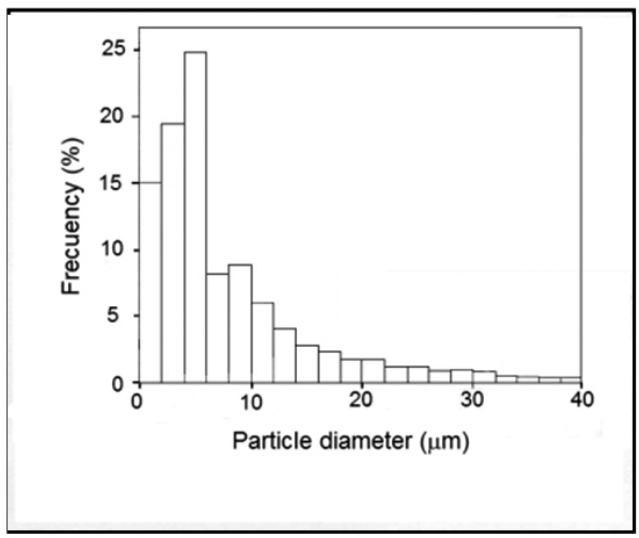

Fig. 2. Distribution of oxide particles in a period of 30 hours of milling.

O_2 electroreduction on $Cu_{1.4}Mn_{1.6}O_4$ by polarization curves.

The size distribution of the pure oxide particles obtained at different grinding and incorporated into CG/PPy(Ox) and CG/CC(Ox) surface were similar.

To specify the Faraday current related to the orr on CG/paint/CC(Ox)/PPy and CG/PPy/PPy(Ox)/PPy composite electrodes, steady-state i-η curves were recorded point by point from 0 to -0.6V as shown in Fig 3.

It can be seen that CG/PPy and CG/PPy/PPy showed a low electrochemical answer in O_2 atmosphere similar to CG/PPy/PPy(Ox)/PPy electrode in Ar atmosphere, showing that the oxide into the CG/PPy/PPy(Ox)/PPy composite electrode was sufficiently stable and it does not decompose at negative overpotentials such as -0.6V. The comparison of the cathodic currents on the CG/PPy/PPy(Ox)/PPy composite electrode with those on the CG/PPy/PPy electrode pointed out that O_2 reduction occurred actually on the oxide particles retained by the polymer. The effect of oxide particle size is remarkable considering the narrow range studied 7.6 - 11.2 µm (Fig 3). The oxygen reduction currents observed on CG/paint/CC(Ox)/PPy composite electrode in air atmosphere were higher than the ones observed on CG/PPy/PPy(Ox)/PPy composite electrode containing the same oxide mass and particles size 7.6 µm (Fig.4). The orr on CG/paint/CC(Ox)/PPy composite electrode shows a limiting current plateau at -0.6V while for CG/PPy/PPy(Ox)/PPy is -0.52V. At same overpotential, the current due to orr on oxide particles confined in carbon cloth is much faster than the particles confined on PPy layer using the

same oxide mass and particle diameter, perhaps due to two combined effects: high electric conductivity and high oxygen diffusion process in the case of CC.

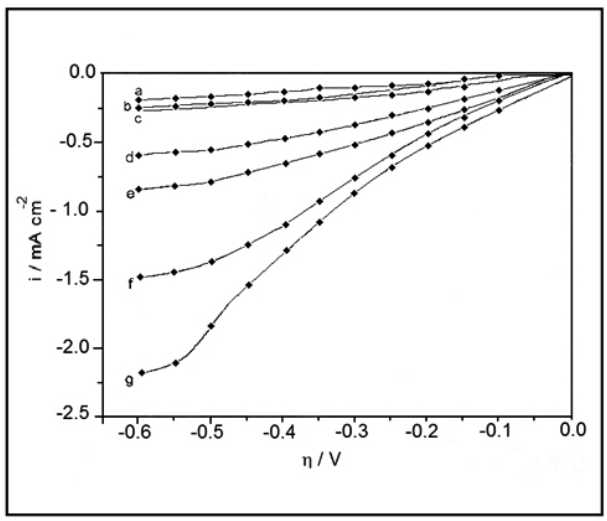

Fig. 3. Steady state polarization curves of O_2 reduction on a) CG, b) GC/ PPy, d) GC/PPy/PPy(Ox)/PPy electrode with oxide particles size of 11.2 µm, e) 9.6 µm, f)8.5 µm, g) 7.6 µm , KCL solution, p_{O2}= 1 atm, RT, c) GC/PPy/PPy(Ox, 7.6 µm)/PPy electrode in Ar.

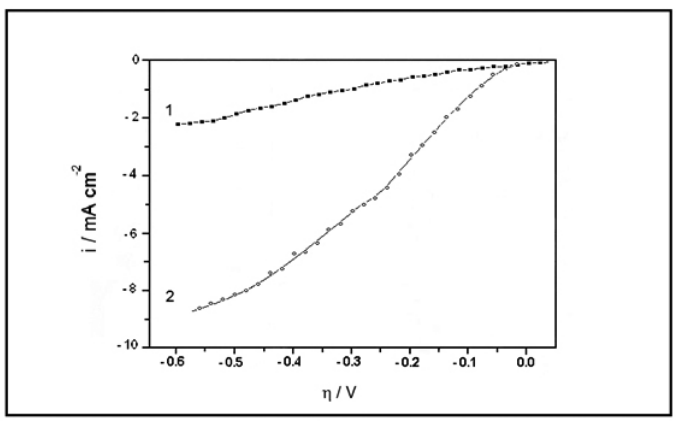

Fig. 4. Polarization curves of orr on (1) GC/PPy/PPy(Ox, 7.6 µm)/PPy, (2) GC/paint/CC(Ox, 7.6 µm)/PPy electrodes.

As it was expected, the orr current densities on the composite electrodes depends simultaneously on the overpotential reaction and particle size of the catalyst as shown in Fig 5.

The stability of the composite electrodes was examined potentiostatically at -0.4V in 0.2 M KCl solution, p_{O2} = 1 atm at RT during 1.5 h using composite CG/paint/CC, CG/paint/CC/PPy and CG/PPy/PPy electrodes without oxide. It was found a very low current density for all cases (~ 0.1 mAcm^{-2}) showing the high stability of these interphases.

Electroreduction of O_2 on $Cu_{1.4}Mn_{1.6}O_4$ using ring-disk electrode technique

.Different complex mechanisms have been proposed for the orr depending on the nature of the electrocatalyst, electrolyte and pH.[28]. It can be considered the following reaction pathways: direct pathway $O_2 + 2H_2O + 4e \rightarrow 4OH^-$ (E = -0401 V/SHE) with kinetic constant k_1 and indirect pathway $O_2 + HO_2^- + 2e \rightarrow HO_2^- + OH^-$ (E = -0.065 V/SHE) with kinetic constant k_2, followed by $HO_2^- + H_2O + 2e \rightarrow 3OH^-$ (E = - 0.0867 V/SHE) with kinetic constant k_3. Additionally it is possible to accept a catalytic chemical decomposition of HO_2^- on the oxide surface, $HO_2^- \rightarrow OH^- + ½\ O_2$ with kinetic constant k_4. The peroxide ions, HO_2^-, which are formed on the disk electrode, can be reoxidized on the ring electrode according to reaction: $HO_2^- + OH^- \rightarrow O_2 + H_2O + 2e$. The equations which describe the process are:

$-N\ (I_D/I_R) = [1 + (2k_1/k_2)] + (1/Z_{HO2^-}\ \omega^{1/2})[2k_1(k_3+k_4)/k_2 + (2k_3+k_4)] = J_1 + S_1\ \omega^{-1/2}$ (1)

$-N\ (I_{D,L} - I_D)/\ I_R = n_D/2[D_{02}/D_{HO2^-}][(k_3+k_4)/k_2] + n_D/2\ (Z_{O2}\ \omega^{1/2}/k_2) = J_2 + S_2\ \omega^{1/2}$ (2)

with $Z_i = 0.62\ D_i^{2/3}\ \nu^{-1/6}$ and $I_{D,L} = -n_D F A_D\ Z_{O2}(k_1+k_2)C_{O2}$, where N is the collection efficiency of the ring electrode, I_D and I_R are the disk and ring electrode currents of opposite signs, ν the kinematic viscosity, C_{O2} the oxygen concentration, D_i is the diffusion coefficient of species i (i being O_2 or HO_2^-), n_D the mean number of electrons per oxygen molecule transferred at the disk electrode and ω is the electrode rotation rate.

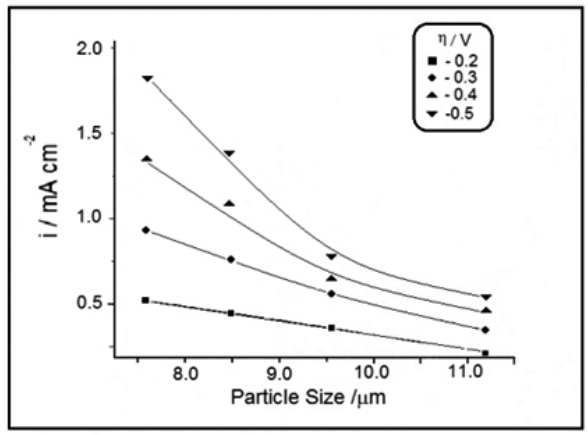

Fig. 5. Dependence of orr current on overpotential applied and oxide particles size.

The k_1/k_2 ratio can be obtained from the extrapolated ordinate (J_1) at ω = 0 of $-N\ (I_D/I_R)$ against $\omega^{-1/2}$ plot (Equation 1), and k_2 from the slope (S_2) of $-N\ (I_{D,L} - I_D)/I_R$ against $\omega^{1/2}$ plot (Equation 2). From these values, it is possible to determine whether the orr proceeds via the direct reduction pathway (four electrons), via the indirect reduction pathway, in two steps (2 + 2 electrons) or simultaneously via both pathways (parallel mechanism) with predominance of one or the other pathway.

Figure 6 shows the steady state η/I curves between 0 to -05 V in O_2 saturated solution for different rotation rate between 500 to 3000 rpm. It is clear that the currents (I_D and I_R) increase with rotation rate. In both cases the currents at the disk electrode, I_D, and at the ring electrode, I_R, were higher than those obtained in Ar (not shown) principally due to oxygen reduction to HO_2^-. Only one oxygen reduction vague is observed, indicating that the graphite containing in the pellet or in the cloth does not participate in the electrocatalytical reaction.

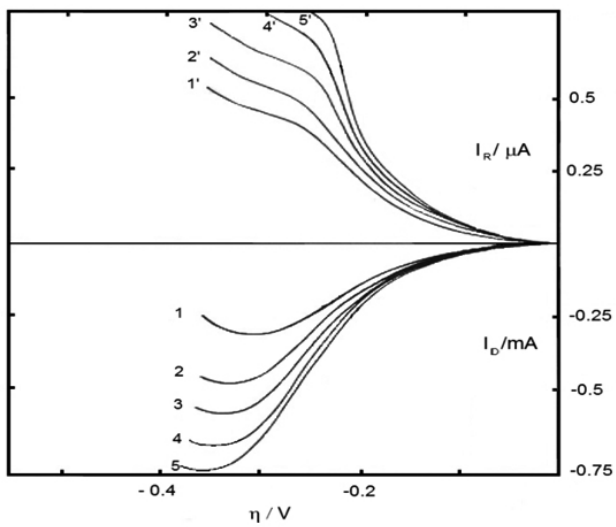

Fig. 6. Disk currents and ring currents corresponding to oxygen reduction on G/paint/CC($Cu_{1.4}Mn_{1.6}O_4$,7.6 µm)/PPy in 0.2M KCl, pH = 9, O_2 saturated solution, RT at different electrode rotation rate. (1,1′) 500 rpm, (2,2′) 1000 rpm, (3,3′) 1500 rpm, (4,4′) 2500 rpm, (5,5′) 3000 rpm.

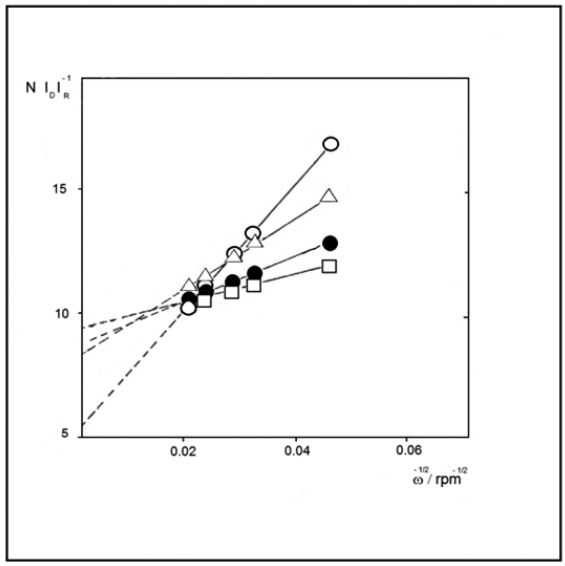

Fig. 7. $N(I_D/I_R)$ vs. $\omega^{-1/2}$ relationship for various overpotentials applied. (o) -0.22V, (Δ) -0.2V, (•) -0.18 V, (□) -0.15V.

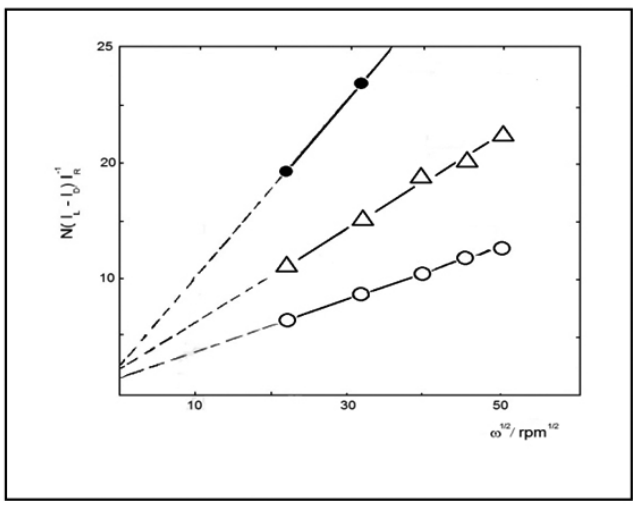

Fig. 8. $N(I_L-I_D)/I_R$ vs. $\omega^{1/2}$ relationship for various overpotentials applied. (•) -0.15V, (Δ) – 0.18V, (o) -0.2 V.

Figure 7 shows straight line $-N(I_D/I_R)$ vs. electrode rotation at different overpotentials. It can be seen that the slope increases and decreases the intercept with increasing overpotential, showing that k_1/k_2 ratio increases as the overpotential becomes more negative. Considering that the slope is positive, it appears that the peroxide ions formed are then decomposed. From the graph $-N(I_{D,L} - I_D)/ I_R$ vs. $\omega^{1/2}$ (Fig. 8) it can be seen that the HO_2^- reduction reaction to OH^- is very sensitive to the applied overpotential.

To determine the effect of electrocatalyst particle size on the hydrogen peroxide formation kinetics, CG/PPy/PPy(Cu1.4Mn1.6O4)/PPy composite electrodes containing different oxide particles size were potentiostatically polarized at -0.55V in 0.2M KCl solution, O_2 saturated, for 80 min. Figure 9 shows that oxide particles size have an important effect on HO_2^- ions formation, consequence of the electrocatalyst surface area.

4. Chemical decomposition of hydrogen peroxide

As indicated above, it is possible that the HO_2^- ion decomposes chemically on the surface oxide $Cu_{1.4}Mn_{1.6}O_4$. Figure 10 shows the results concerning the decrease of hydrogen peroxide concentration generated electrocatalytically at different particles size (t = 0). It can be observed that HO_2^- ion concentration decreases as function of time in all cases, being higher with smaller particles than bigger particles at 60 minutes.

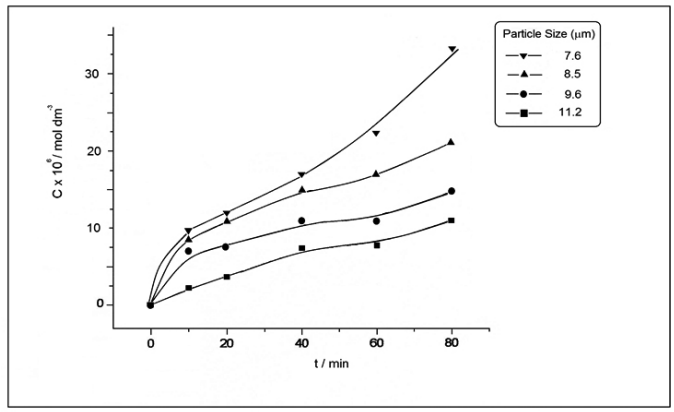

Fig 9. Hydrogen peroxide concentration vs. reaction time during orr on CG/PPy/PPy($Cu_{1.4}Mn_{1.6}O_4$)/PPy composite electrode as a function of oxide particles size

CONCLUSIONS

This work shows that the direct incorporation into polypyrrole matrix or into high-surface area carbon cloth of $Cu_{1.4}Mn_{1.6}O_4$ particles having spinel structure can be used as stable electrocatalyst for oxygen reduction reaction. The O_2 electroreduction occurs with hydrogen peroxide formation as intermediate species of a 2 + 2 electrons mechanism. The size of the oxide particles plays an important role in both important processes: the electrocatalytic hydrogen peroxide formation as well as in their chemical decomposition.

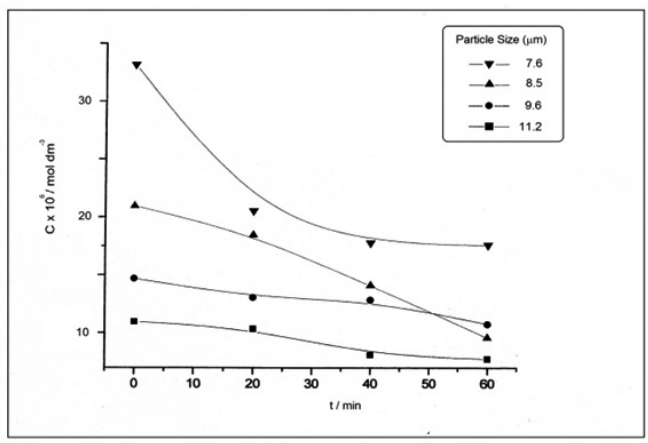

Fig 10. Chemical hydrogen peroxide decomposition on the time as a function of oxide particles size.

ACKNOWLEDGEMENTS

In memory at Dr. Luis Nuñez. This paper was partially supported by DICYT (Universidad de Santiago) and CIAM 20001 (CONICYT). JO and JLG thanks Dr M. Cazanga for the cooperation.

REFERENCES

1. H.Meng, P.K.Sen, *Electrochem. Commun*. **8**, 588, (2006)
2. D.Capsoni, M.Bini, S.Ferrari, E.Quartarone, P.Mustarelli, *J. Power Sources* **220**, 253, (2012)
3. M.Panizza, G.Cerisola, *Water Research* **35**, 3987, (2001)
4. G.Wu, K.More, C.M.Johnston, P.Zelenay, *Science* **332**, 443, (2011)
5. M.S. El-Deab, T.Osaka, *Electrochim. Acta* **52**, 2166, (2007)
6. S.Trasatti in Electrochemistry of Novel Materials, J.Lipkowski and P.N.Ross eds.,Wiley-Vch, N.Y., 1994; pp. 207-294

7. J.Ortiz and J.L.Gautier in Electroquímica y electrocatálisis. Materiales: aspectos fundamentales y aplicaciones, N. Alonso-Vante ed. e-libro net. Bs Aires, 2003; pp.132-214
8. H.N. Cong, K. El Abbassi, P. Chartier, *J. Electrochemical Soc*. **149**, A525, (2002)
9. H.N.Cong, V. de la Garza Guadarrama, J.L.Gautier, P. Chartier, *J. New Mat. Electrochem. Systems* **5**, 35,(2002)
10. H.N.Cong, V. de la Garza Guadarrama, J.L.Gautier, P.Chartier, *Electrochim. Acta* **48**, 2389, (2003)
11. R.N.Singh, B.Lal, M.Malviya, *Electrochim. Acta* **49**, 4605, (2004)
12. J.L.Gautier, A.Restovic, G.Poillerat, P.Chartier, *Eur. J. Solid State Inorg. Chem. **34***, 367 (1997)
13. H.N.Cong, K. El Abbassi, J.L.Gautier, P.Chartier, *Electrochim. Acta* **50**, 1369, (2005)
14. E. Ríos, S. Abarca, P. Daccarett, H .N. Cong, D. Martel, J. F. Marco, J.R. Gancedo, J.L. Gautier, *Int. J. Hydrogen Energy* **33**, 4945, (2008)
15. J.F. Marco, J.R. Gancedo, H.N. Cong, M. del Canto, J.L. Gautier, *Solid State Ionics*, **177**, 1381, (2006)
16. J.F. Marco, J.R. Gancedo, H.N. Cong, K. El Abbassi, M. del Canto, E. Ríos, J.L. Gautier, *Mat. Res. Bull.* **43**, 2413, (2008).
17. E. Frackowiak, F. Béguin, *Carbon*, **39**, 937, (2001)
18. K.H. An, W.S.Kim, Y.S. Park, Y.C.Choi, S.M. Lee, D.C. Chung, D.J.Bae, S.C. Lim, Y.H. Lee, Adv. Mater., **13**, 497, (2001)
19. C.V. Guteri, S.Saadallah, K. Jurewicz, E. Frackowiak, M. reda, J. Parmentier, J. Patarin, F. Beguin, *Mat. Sci. Eng. B,* **108**, 14, (2004)
20. Y.G. Wang, X.G. Zhang, *Electrochim. Acta* **49**, 1957, (2004)
21. T.N. Ramesh, P.V. Kamath, C. Shivakumava, *J. Electrochem. Soc.,* **152**, A871, (2005)
22. H.K. Xin, W.Q.Fu, Z.X. Gang, W.X. Lei, *J. Electrochem. Soc.,* **153**, A1568, (2006)
23. M.Yaldagard, M.Jahanshahi, N. Seghatoleslami, *World J. Nano Sc. And Eng.***3**, 121, (2013)
24. R.A. Davoglio, S.R.Baggio, N.Bocchi, R.C. Rocha-Filho, *Electrochim. Acta*, **93**, 93, (2013)
25. D. Zhang**,** H. Yan**,** Y. Lu, K. Qiu, Ch. Wang, Ch. Tang, Y. Zhang**,** Ch. Cheng**,** Y. Luo, *Nanoscale Res. Lett*. **9**, 139, (2014)
26. H.N.Cong, Y. Shao, *Solid State Ionics* **178**, 1385, (2007)
27. T.J. Collins, *BioTechniques* **43** (1 25 (2007)
28. K. Kinoshita, Electrochemical Oxygen Technology, J.Wiley , N.Y. 1992.